Composition of lipids from the First Lusatian lignite seam of the Konin Basin (Poland): relations to vegetation, climate and carbon cycling during the mid-Miocene Climatic Optimum

A. Bechtel [1], M. Widera [2], M. Woszczyk [3]

[1] Applied Geosciences & Geophysics, Montanuniversität Leoben, Peter-Tunner-Strasse 5, A-8700 Leoben, Austria
[2] Adam Mickiewicz University, Institute of Geology, 12 Krygowski Street, 61-680 Poznań, Poland
[3] Adam Mickiewicz University, Laboratory of Biogeochemistry,10 Krygowski Street, 61-680 Poznań, Poland

Geological Setting and Samples

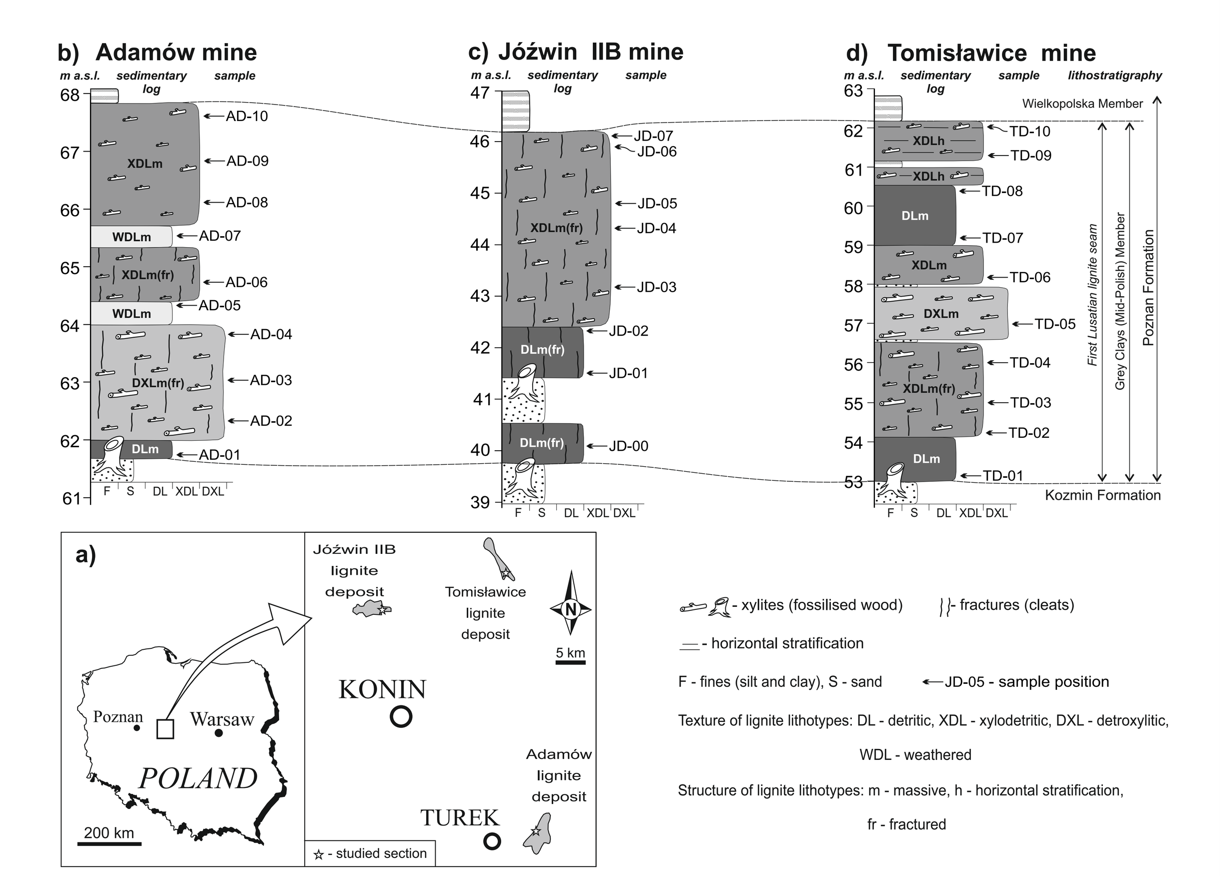

Fig. 1: (a) Location of the studied lignite opencast mines in the Konin Basin (Poland); and lignite lithotypes, structural elements, and position of detrital lignite samples in the profiles from the (b) Adamów, (c) Jóźwin IIB, and (d) Tomisławice opencast mines.

The Adamów, Jóźwin IIB and Tomisławice lignite mines cover fault-bounded, relatively shallow tectonic depressions. They are located ~20–35 km of Konin in central Poland (**Fig. 1a**). The Grey Clays Member of the Miocene Poznań Fm. contains the examined First Lusatian lignite seam. It is up to several meters thick, on average 6.3–8.1 m (**Fig. 1b-d**). The seam formed in the middle part of the mid-Miocene (~15 Ma), during the last peak of the mid-Miocene Climatic Optimum.

Bulk geochemistry and molecular composition of lipids

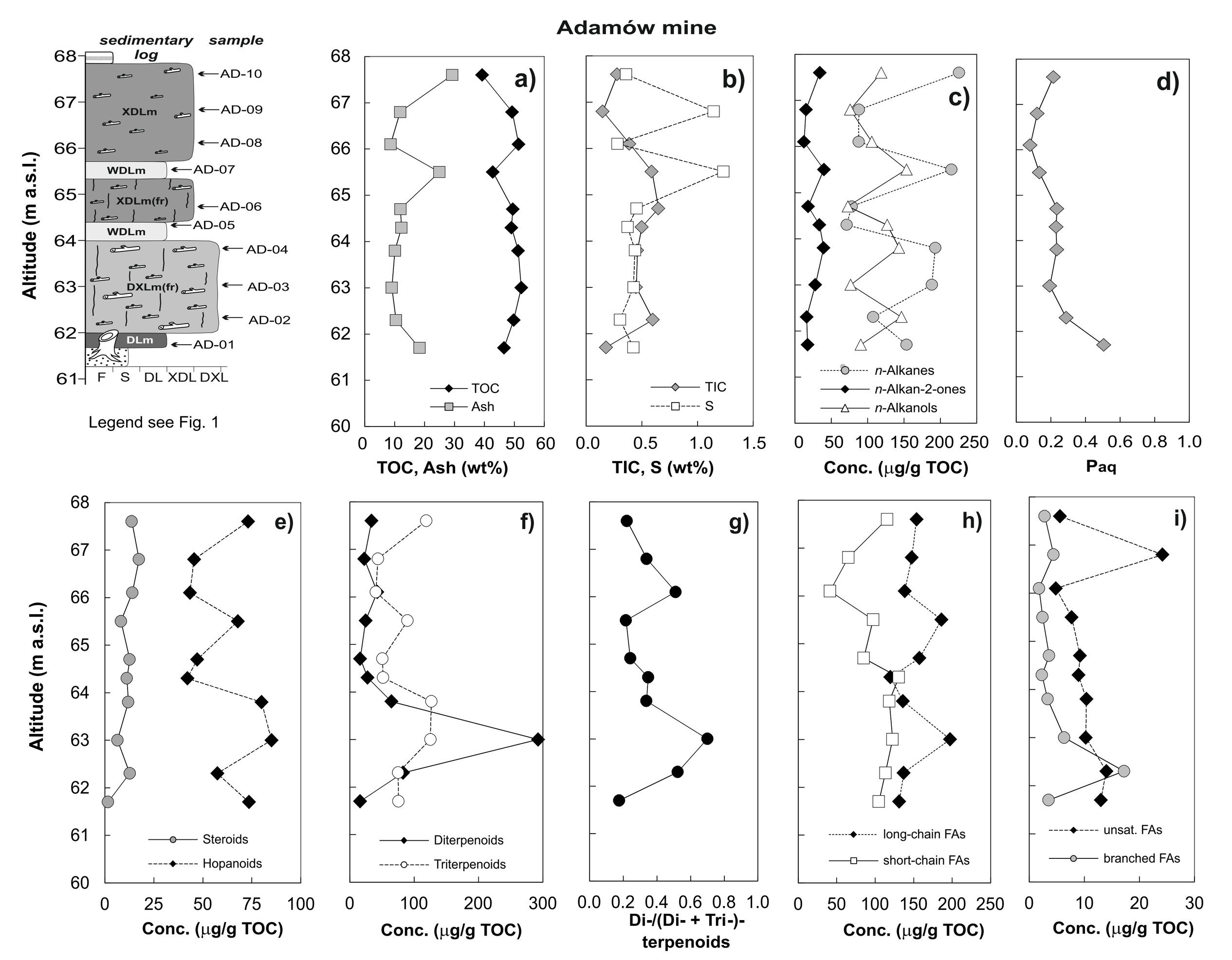

Fig. 2: Sampling position and variation of concentrations and concentration ratios of lipids within the First Lusatian lignite seam at the Adamów mine.

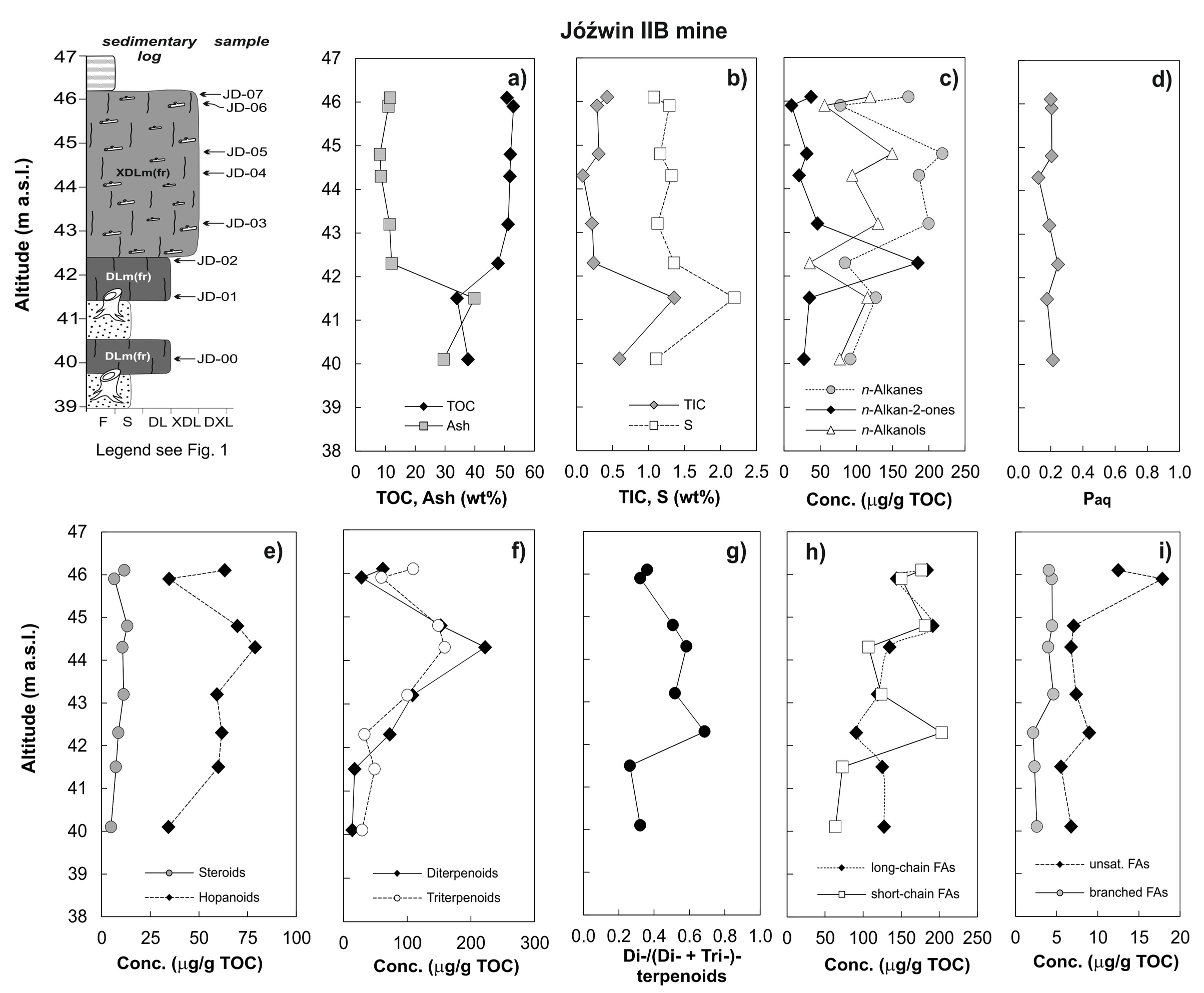

Fig. 3: Sampling position and variation of concentrations and concentration ratios of lipids within the First Lusatian lignite seam at the Jóźwin IIB mine.

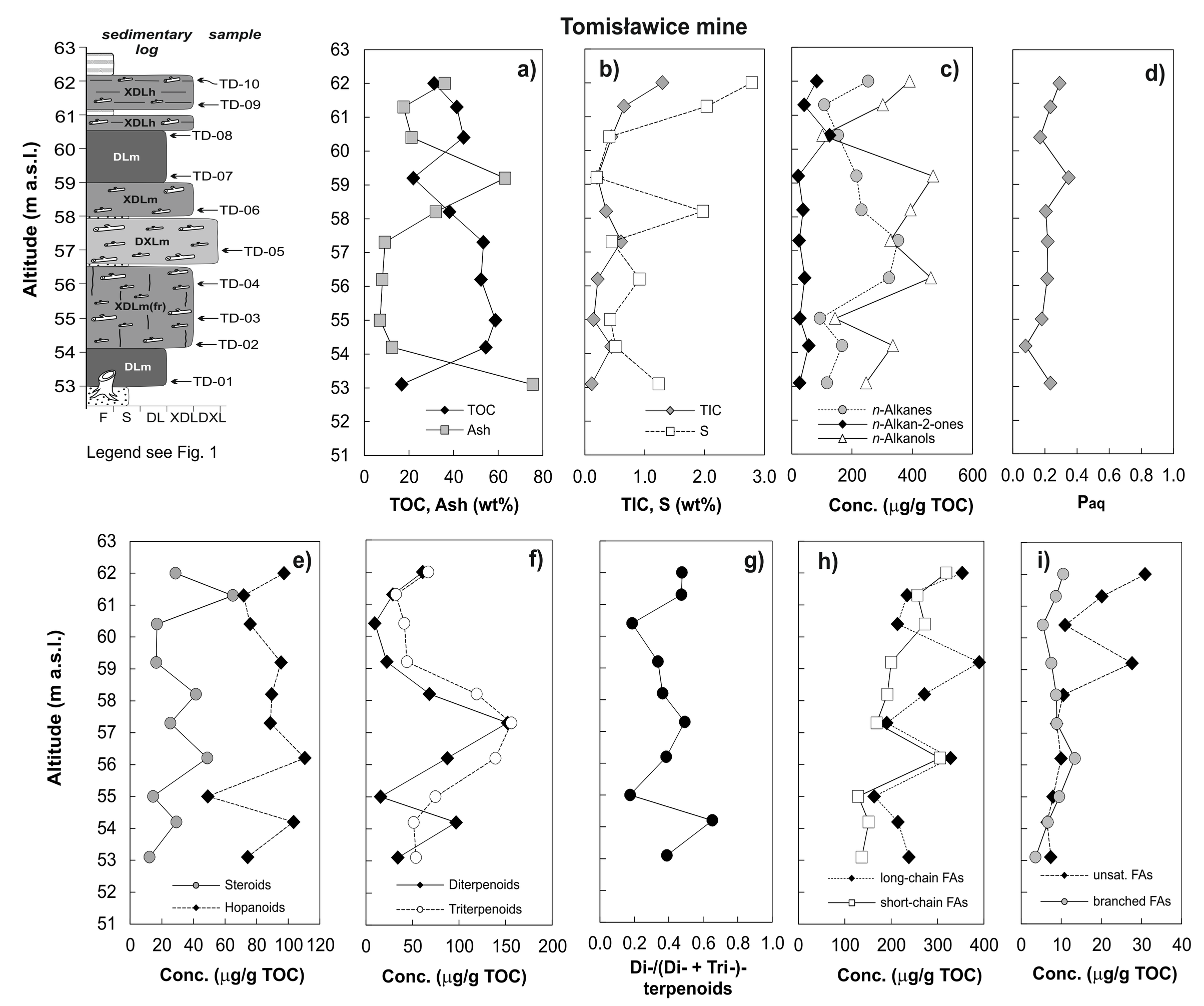

Fig. 4: Sampling position and variation of concentrations and concentration ratios of lipids within the First Lusatian lignite seam at the Tomisławice mine.

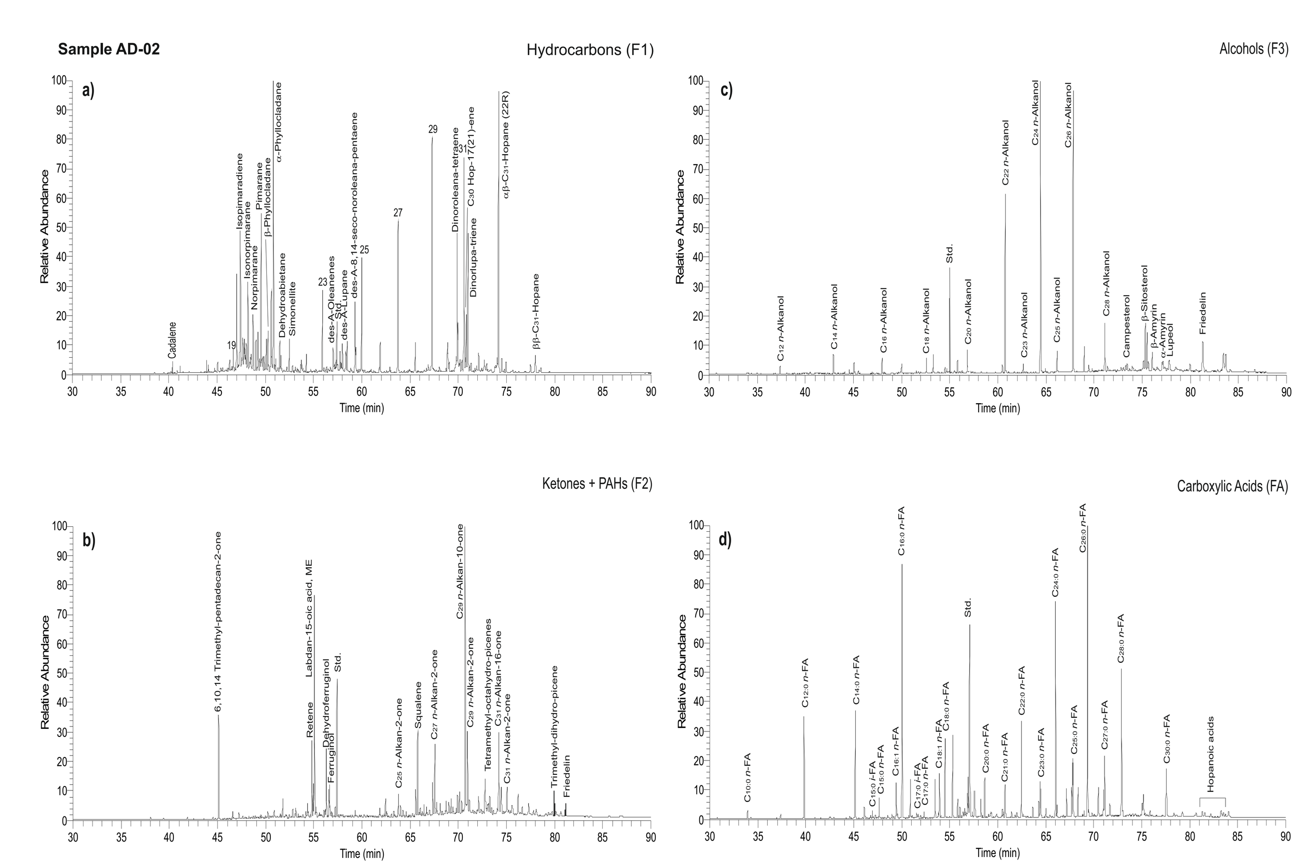

Fig. 5: Total ion current chromatograms of the (a) hydrocarbon fraction, (b) the ketone fraction, (c) the alcohol fraction, and (d) the carboxylic acids obtained from the lignite sample AD-02, Std. = Internal Standard (deuterated tetracosane (F1), 1,1´-binaphthyl (F2), 1-nonadecanol (F3), nonadecanoic acid (FA), respectively).

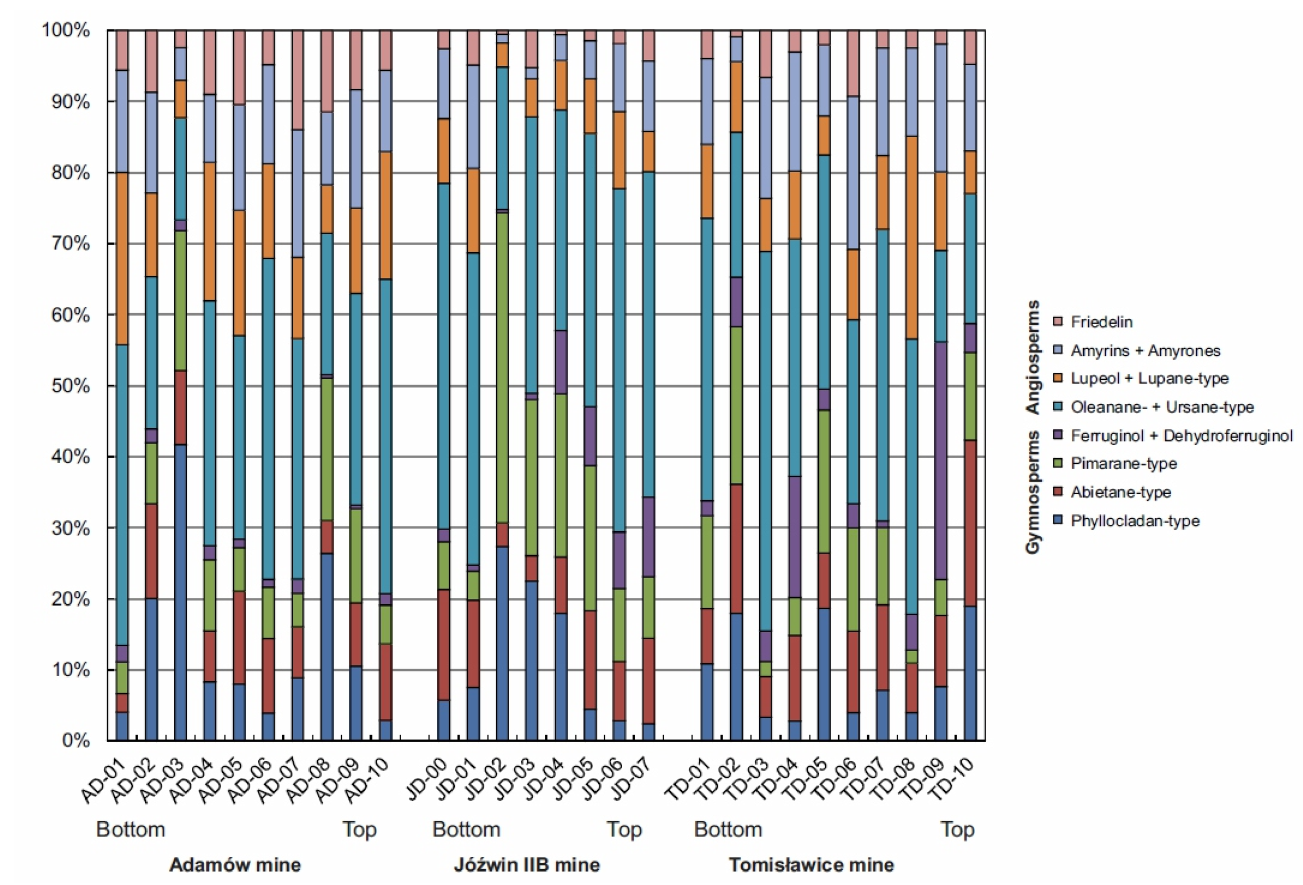

Fig. 6: Relative percentages of source specific plant lipids within the samples.

Elevated ash yields and low sulfur contents indicate peat formation in topogenous mires under freshwater conditions (**Figs. 2, 3, 4**). The molecular composition of the extracted lipids is highly variable, including leaf-wax *n*-alkanes in the C_{23} to C_{31} range, diterpenoids, hopanoids, and angiosperm-derived triterpenoids, as well as saturated fatty acids, long-chain *n*-alkanols and *n*-alkan-2-ones (**Figs. 2, 3. 4**). The enhanced abundances of short-chain n-FAs in several lignite samples argue for the contribution of algae and microorganisms to the biomass during periods of raised water table. Low $\beta\beta/(\beta\beta+\alpha\beta)$ hopane ratios imply acidic conditions during peatification. High concentrations of plant wax derived lipids are found in samples of detrital lignite (**Fig. 5**). The relative abundances (P_{aq} = 0.08–0.51; **Figs. 2d, 3d, 4d**) of mid-chain (C_{23}, C_{25}) *n*-alkanes argue for a minor contribution of macrophytes (graminoids, etc.), enhanced during periods of raised water level. Terpenoid biomarker ratios (**Fig. 6**) argue for mixed vegetation, including gymnosperms (i.e. conifers) and angiosperms. From the sesqui- and diterpenoids present in the lignite (**Fig. 5**), a significant contribution of species of the coniferales families Cupressaceae and Pinaceae is concluded. High relative abundances of triterpenoids of the oleanane and ursane structural types in several parts of the seam indicate angiosperm domination in the peat-forming vegetation (**Fig. 6**). The input from Betulaceae is suggested from the occurrence of lupeol and its derivatives.

Stable Isotope Analyses

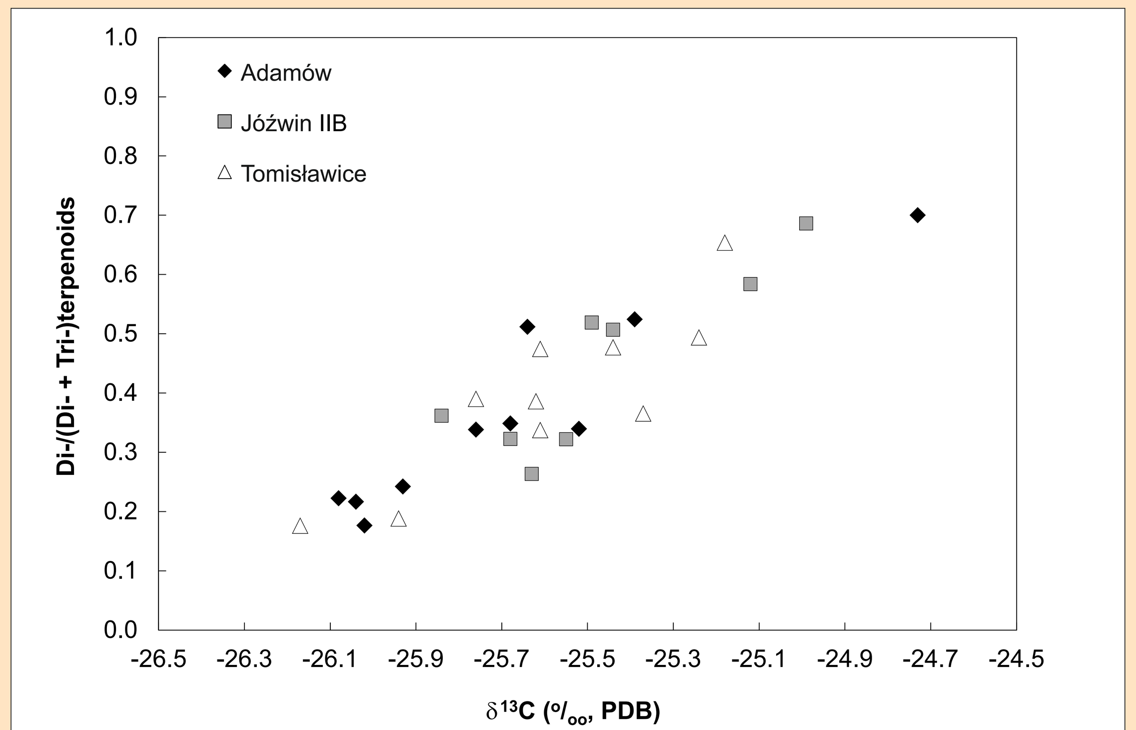

Fig. 7: Cross-correlation of δ13C of total organic carbon versus the ratios of diterpenoids to the sum of di- plus triterpenoids concentrations of lignite samples.

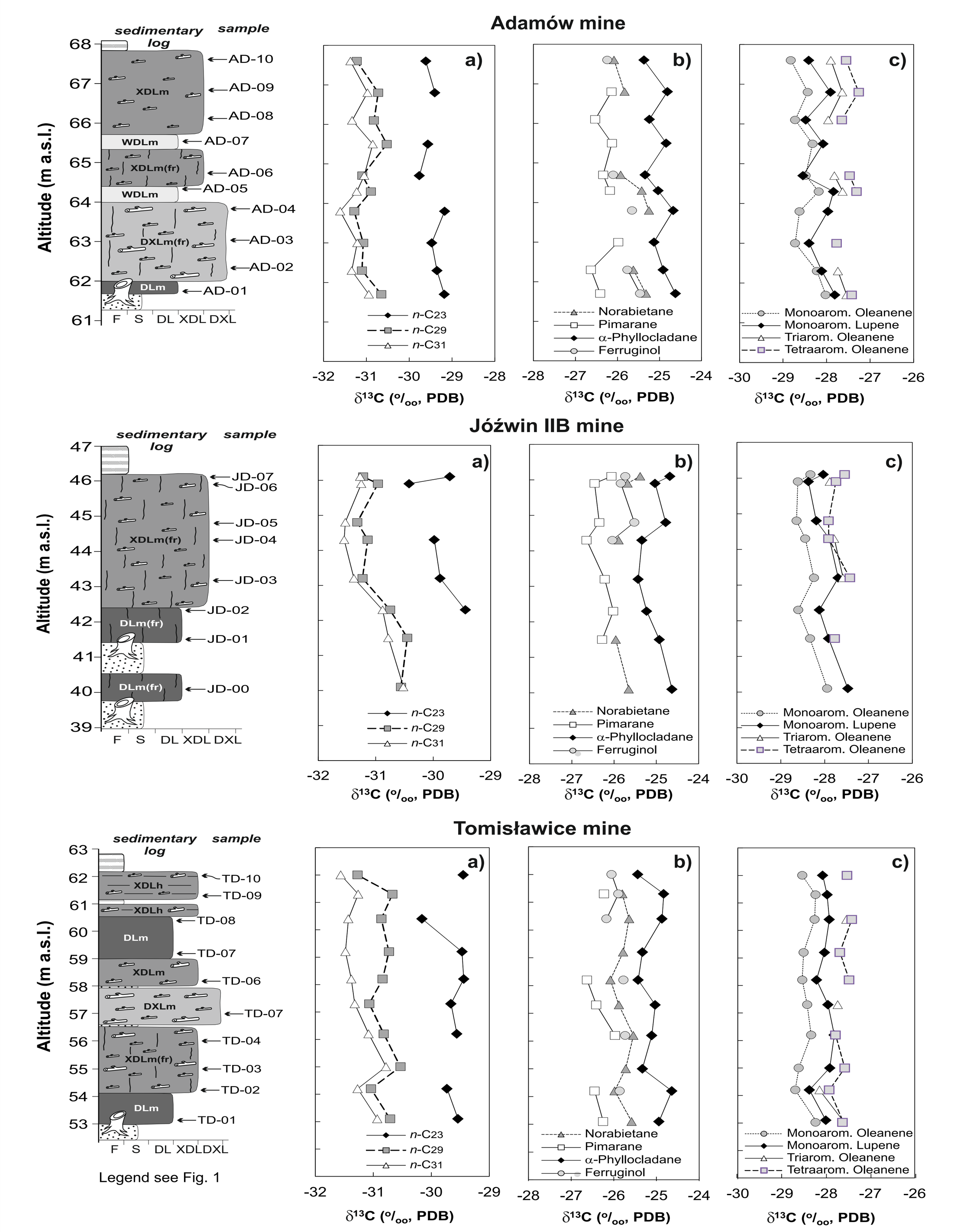

Fig. 8: Depth trends of carbon isotopic compositions of (a) C_{23}, C_{29}, and C_{31} *n*-alkanes, (b) diterpenoids, and (c) triterpenoids within the studied profiles.

The positive correlation between δ13C and di-/(di + tri-)terpenoid ratios of lignite indicates the role of varying gymnosperm/angiosperm contributions on the carbon isotopic composition (**Fig. 7**). The C-isotope data of long-chain *n*-alkanes, diterpenods, and angiosperm-derived triterpenoids show parallel fluctuations within the profiles, arguing for the role of minor variations in δ13C of atmospheric CO_2 on δ13C of plant lipids during the Mid-Miocene Climatic Optimum (**Fig. 8**). However, the influence of local variations in ambient CO_2 (e.g., the canopy effect) cannot be excluded. Fluctuations in δ13C values of individual compounds may also be related to changes in humidity, air temperature, and carbon cycling within the peat (**Fig. 8**).

Acknowledgement: This poster, presented at the EGU General Assembly 2020 in Vienna, is a contribution to the **Research Project No. 2017/27/B/ST10/00001,** funded by the **National Science Centre, Poland.**

CC BY